

Supplementary File

I. ALGORITHMS

Algorithms 1, 2, 3 and 4 contain pseudocodes of the algorithmic approaches described in this work.

Algorithm 1 Foreground Extraction of cropped video frame from cluttered background.

```

1: procedure EDGES( $f_n$ )
2:    $\triangleright f_n$  : cropped window from  $n^{th}$  video frame
3:    $f_h \leftarrow \text{equalizeHist}(f_n)$ 
4:    $f_g \leftarrow \text{GaussianBlur}(f_h)$ 
5:    $f_e \leftarrow \text{Canny}(f_g)$ 
6:   return  $f_e$   $\triangleright f_e$  : the edges of  $f_n$ 
7: procedure MORPH( $f_e$ )
8:    $ker1 \leftarrow \text{kernel}(25 \times 3)$ 
9:    $ker2 \leftarrow \text{kernel}(15 \times 15)$ 
10:   $f_{ed} \leftarrow \text{dilate}(f_e, ker1)$ 
11:   $f_{ee} \leftarrow \text{erode}(f_{ed}, ker2)$ 
12:   $f_{e2} \leftarrow 255 - f_{ee}$ 
13:  return  $f_{e2}$   $\triangleright f_{e2}$  : After dilation, erosion, inversion
14: procedure FOREGROUND( $f_{e2}$ )
15:   $labels \leftarrow \text{CCL}(f_{e2})$ 
16:   $props \leftarrow \text{regionProperties}(labels)$ 
17:   $lbMask \leftarrow \text{zeros}(\text{size}(labels))$ 
18:    $\triangleright$  To contain individual components
19:   $fullMask \leftarrow \text{zeros}(\text{size}(labels))$ 
20:   $\triangleright$  if  $lbMask$  passes tests, it gets added to  $fullMask$ 
  later
21:  while  $lb = \text{unique}(labels)$  do
22:     $\triangleright$  Loop through each labeled component
23:     $cond1 \leftarrow \text{props}(lb).size > 500$ 
24:     $\triangleright$  Condition 1: size > 500 pixels
25:     $cond2 \leftarrow \text{props}(lb).eccentricity > 0.9$ 
26:     $cond3 \leftarrow (\text{props}(lb).orientation > -0.3) \text{ and } (\text{props}(lb).orientation < 0.3)$ 
27:    if  $cond1$  and  $cond2$  and  $cond3$  then
28:       $lbMask \leftarrow \text{convexHull}(lbMask)$ 
29:       $fullMask \leftarrow fullMask + lbMask$ 
30:       $lbMask \leftarrow \text{zeros}(\text{size}(labels))$ 
31:  return  $fullMask$   $\triangleright$  Returns the foreground

```

II. DESIGN OF 3D PRINTED FIELD ROBOT

Heavy weight equipment damages the agricultural ecosystem by increasing soil compaction, which can significantly reduce yield [1]. Soil compaction reduces the ability of the soil to drain quickly and prevents rapid progression of roots, leading to damage to plants due to retained water and

Algorithm 2 Camera motion estimation using dense optical flow (structure from motion).

```

1: procedure OPTFLOW( $f_n, V_R$ )
2:    $\triangleright f_n$ : window for  $n^{th}$  video frame,  $V_R$ : instantaneous robot velocity
3:    $(V_x, V_y) \leftarrow \text{denseOpticalFlow}(frame, 10)$ 
4:    $\triangleright$  For 10 consecutive frames
5:    $R \leftarrow V_R / V_x$   $\triangleright V_x$ : motion in horizontal direction
6:   return  $R$   $\triangleright$  Ratio to be used for width calculation

```

Algorithm 3 Lateral distance estimation from filtered points using 2D LIDAR

```

1: procedure ESTIMATELATERALDISTANCE()
2:    $Pt_{filt} \leftarrow \text{ProcessLidarData}(V_l, Lim)$ 
3:    $\triangleright$  For filtering data.  $V_l$  is the array of all LIDAR points,  $Lim$  is the lower and upper limits,  $Pt_{filt}$  is the array of filtered points
4:   for  $side \in \mathcal{S}$  do  $\triangleright \mathcal{S}$  contains left or right side
5:      $Pt_{side} \leftarrow \text{SplitSides}(Pt_{filt}, Lim_{side})$ ;
6:      $(Pt_{chosen}, numP) \leftarrow \text{ChooseByHist}(Pt_{side})$ 
7:      $\triangleright$  choose best fit line according to histogram
8:      $Fit \leftarrow \text{getLine}(Pt_{chosen})$ 
9:      $Prev \leftarrow (D_{lat}, \theta_r)$   $\triangleright D_{lat}$  is lateral distance and  $\theta_r$  is the row angle
10:     $(Len, D_{lat}, \theta_r, SD, Df) \leftarrow \text{LineInfo}(Fit)$ 
11:     $\triangleright SD$  is standard deviation of points,  $Df$  is difference,  $Len$  is the length
12:     $W_{lane} \leftarrow \text{Sum of lateral distances}$ 
13:     $LineGrade(\mathcal{S}) \leftarrow \text{Eval}(NumP, Len, SD, Df)$ 
14:     $D \leftarrow \text{LineGrade}(S_{right})$   $\triangleright D$  is the lateral distance towards right, that is later used for width estimation
15:  return  $D$ 

```

slowed or stunted growth. It is widely accepted that lightweight equipment is preferred, and has been shown to lead to better yields. However, heavy weight machinery made out of metal parts is widely used in agriculture because of its perceived structural strength. Indeed, when the job of the equipment is to pull heavy weight, such as for plowing, harvesting, or tilling, heavy weight equipment make a lot of sense, but when the job of the equipment is to carry a few sensors, an entirely different approach that leads to extremely lightweight platforms is possible. In this paper, we utilize this viewpoint to develop a novel robot that is constructed entirely out of 3-D printed construction. This leads to an extremely light-weight robot (14.5 lbs), yet, the robot has been proven to be structurally resilient to field conditions during an entire

Algorithm 4 Width Estimation

```
1: procedure PIXELWIDTH( $fullMask, N$ )
2:    $\triangleright fullMask$ : Output from Algorithm 1
3:    $i \leftarrow N$ 
4:   while  $i > 0$  do
5:      $W_{P_i}[i] \leftarrow CountWhitePixels(col[i])$ 
6:      $\triangleright col[i]$ : column numbers for width calculation
7:      $i \leftarrow i - 1$ 
8:   return  $W_{P_i}$ 
9:
10: procedure SFMWIDTH( $W_{P_i}, R$ )
11:    $\triangleright R$ : output from Algorithm 2
12:    $W_{S_i} \leftarrow W_{P_i} \times R$ 
13:    $W_S \leftarrow sum(W_{S_i})$ 
14:   return  $W_S$   $\triangleright W_S$ : average width from SFM
15:
16: procedure LIDARWIDTH( $W_{P_i}, D, F$ )
17:    $\triangleright D$ : output from Algorithm 3,  $F$ : focal length of
    camera
18:    $W_{L_i} \leftarrow W_{P_i} \times D / F$ 
19:    $W_L \leftarrow sum(W_{L_i})$ 
20:   return  $W_L$   $\triangleright W_L$ : average width from LIDAR
```

season of heavy operation in Corn, Sorghum, and Soybean farms in Illinois. We posit that this robot is an example of the potential of additive manufacturing (3-D printing) in creating a new class of agricultural equipment that works in teams to replace, minimize, or augment traditional heavy farm equipment. In addition, lightweight equipment has several benefits, it is easier to manage, has better endurance, safer to operate in general, and leads to lower ownership cost.

A. Mechanical Design

Figure 1 depicts a CAD drawing of the robot with a suite of sensors attached. The robot has been designed specifically to be ultralight (less than 15lbs) and compact. The ultralight nature of the robot ensures that it does not drive plants into the ground due to its weight, and minimizes the driving momentum of the robot. Most agricultural robots in the literature are significantly heavier. The ultralight design requires significant thought in the selection of material, the construction of the material, and the structural design. Conventional methods for manufacturing agricultural equipment often use metal; however, metal is heavy and expensive. As a stark contrast, our robot is built through novel mechanisms of additive manufacturing, a method of manufacturing which heats and extrudes a thermoplastic filament to produce a three-dimensional object. This novel mechanism has not yet been used to design agricultural robots. Additive manufacturing creates complex designs by layering material, as opposed to traditional metal working, or traditional injection molding of plastics. By leveraging the capabilities of additive manufacturing, the aim is to develop novel designs that minimize the weight while maintaining sufficient structural rigidity. These design features allow us

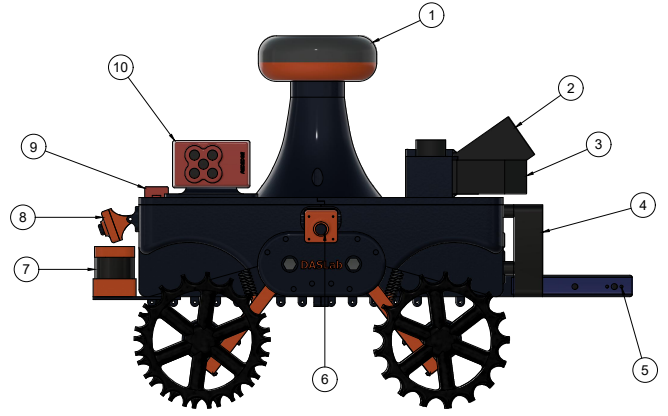


Fig. 1: CAD drawing of the ultra-compact 3D printed robot with a suite of sensors. 1. GNSS antenna, 2. Bayspec hyperspectral sensor, 3. Bayspec hyperspectral sensor (sideward facing), 4. Radiator for the liquid cooling system, 5. Mount for 3d Sensor Intel RealSense, 6. Embedded visual sensor, 7. LIDAR sensor, 8. Embedded visual sensor, 9. GNSS mount for RedEdge multispectral sensor, 10. RedEdge multispectral sensor.

to design a robot that optimally distributes stress and controls the infill percentage allowing for increased strength and durability while being lightweight. Mechanical parts are denser and stronger allowing non-load bearing components to be much lighter. In addition, the design implements specific low-weight metal components, which are carefully selected to maximize the robots field-endurance. Another challenge is ensuring the ground clearance of the robot is sufficiently high to enable traversing complex terrain. The challenge here is with placement. Specifically, motors need to be placed sufficiently close to the robot wheels, to minimize the loss in transmission and to keep it mechanically simple meanwhile, the placement of the motors must allow the robot to operate through continued use in harsh field conditions. This is achieved by creating novel near wheel mechanisms that ensure minimal stress on the motors. Power is transmitted directly to the wheels with as little gears and transmission system as possible to minimize losses.

B. Wheel Design

Appropriate wheel design is critical in ensuring the robot can navigate over crops without damaging them, and navigate over wet and muddy terrains. 3D printing allows us to test many different tread designs to determine optimal tread patterns for the environment. We use flexible filament which has similar properties to rubber while still being able to optimize the design of the tread. The wheels use spade-like arrangements that are designed to provide traction on loose soils while minimizing contact area. As opposed to tracked robots, this wheel design has significant advantages:

- The design does not lead to a large area subject to pressure and force as the robot moves; instead, the wheel design is limited to a small contact area,

- The design is much simpler to manufacture and operate in the field,
- The design is modular, in the sense that each wheel can be replaced if it breaks, instead of having to replace the whole track.

The driving mechanism includes motors mounted near each wheel to enable four independently driven wheels without the need to distribute power from a central power unit. Such a driving mechanism is distinct from existing equipment and vehicles, which utilize a single power plant to transmit power to different wheels. The four-wheel-drive mechanism enables the robot to turn by varying the speeds of independent wheels and is a much simpler mechanism because it does not require complex rack-and-pinion or other similar mechanisms for driving. Another feature of the wheel and mount design is embedding the suspension without having to increase the size of the robot. The suspensions are embedded between the wheel mount and the chassis. The broad chassis provides a simple mechanism that can easily handle bumpy agricultural fields.

C. Hardware

One global navigation satellite system (GNSS) antenna has been mounted straight up the center of the 3D printed robot, and the dual-frequency GPS-capable real-time kinematic differential GNSS module (Piksi Multi, Swift Navigation, USA) has been used to acquire centimeter-level accurate positional information at a rate of 5 Hz. Another antenna and module have been used as a portable base station and has transmitted differential corrections. The placement of hardware is illustrated in Fig. 3. A 3-axis gyroscope (STMicroelectronics L3G4200D) has been used to obtain yaw rate measurement with an accuracy of 2 degrees per second at a rate of 5 Hz. There are four brushed 12V DC motors with a 131.25:1 metal gearbox (Pololu Corporation, USA), which are capable of driving an attached wheel at 80 revolutions per minute. A two-channel Hall-effect encoder (Pololu Corporation, USA) for each DC motor is attached to measure velocities of the wheels. The Sabertooth motor controller (Dimension engineering, USA) is a two channel motor driver that uses digital control signals to drive two motors per channel (left and right channel) and has a nominal supply current of 12 A per channel. The Kangaroo x2 motion controller (Dimension engineering, USA) is a two channel self-tuning PID controller that uses feedback from the encoders to maintain desired linear and angular robot velocity commands. An onboard computer (1.2GHz, 64bit, quad-core Raspberry Pi 3 Model B CPU) acquires measurements from all available sensors and sends desired control signals (e.g., desired linear and angular velocities) to the Kangaroo x2 motion controller in the form of two Pulse-width modulation signals. The block diagram of hardware is illustrated in Fig. 2. All available measurements from all its onboard sensors (GNSS, gyroscope, and encoders) are fed to an online state and parameter estimator to estimate yaw angle of the robot and traction parameters. In every time instant, estimates are updated and fed to the trajectory

tracking controller which calculates the desired angular velocity to follow the reference path given by a trajectory generator. The desired angular and linear velocities are then sent to the Kangaroo x2 Motion Controller as reference command signals in the form of the Pulse-width modulation signal. The Kangaroo x2 Motion Controller functions as the robot's low-level controller by using feedback from encoders attached to the motors to determine the required control signals for tracking the given reference command signals to ensure that the robot's desired velocities are maintained. The Kangaroo x2 Motion Controller outputs the modified command signals to the Sabertooth Motor Controller (SMC) which correlates the given control signals to the necessary output voltages needed by the DC motors. Images are recorded with an RGB digital camera (ELP USBFHD01M, USA) mounted on the side the robot chassis. The field of view of the camera is 60°. The number of corn plants captured in the image depends on the distance between the camera and plant row, as well as the spacing between adjacent plants. In a 30-in row, for instance, two to three corn plants normally appear in the image. The camera points down at an angle of 35° to avoid observing corn rows far away. The resolution of the camera is 640 × 480, and it records at 30 frames per second. The camera has a USB 2.0 interface that connects to a Jetson TX2 (NVIDIA, USA), an embedded module for fast and efficient deep neural network inference. The module houses 8GB memory that is shared between CPU and GPU, and is able to process image frames captured by the camera in real-time.

REFERENCES

- [1] P. Andrade-Sanchez, M. A. Gore, J. T. Heun, K. R. Thorp, A. E. Carmo-Silva, A. N. French, M. E. Salvucci, and J. W. White, "Development and evaluation of a field-based high-throughput phenotyping platform," *Functional Plant Biology*, vol. 41, no. 1, pp. 68–79, 2014.

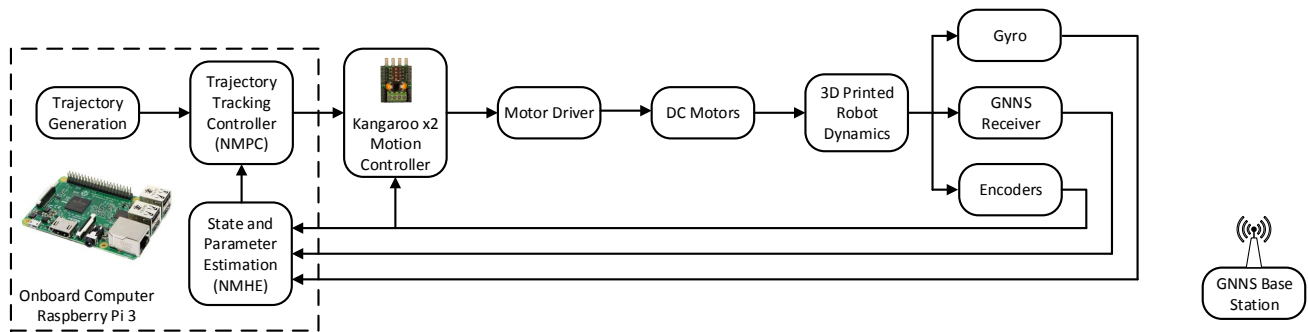


Fig. 2: Block diagram of the hardware

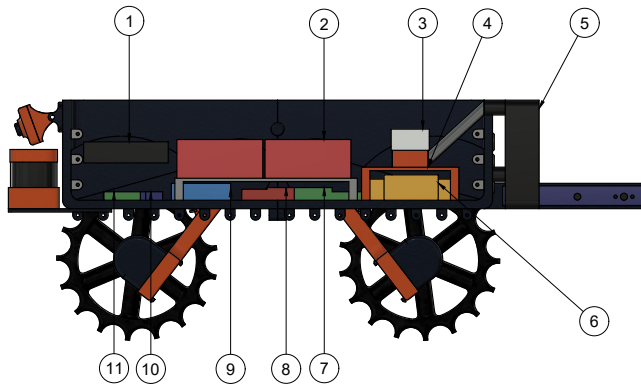


Fig. 3: Interior of the ultra-compact 3D printed robot. 1. Raspberry Pi, 2. Lithium Ion Batteries, 3. Tegra, 4. Heat sink, 5. Cooling Fan, 6. Kangaroo/Sabertooth, 7. Regulator, 8. 3-axis gyroscope, 9. Breadboard, 10. Raspberry Pi C.